Stimuli responsive surfactants: towards smart templates for mesoporous silica nanoparticles

Inês Santos, José Paulo Sequeira Farinha[1], Carlos Miguel Calisto Baleizão[1]

1- Supervisor, Instituto Superior Técnico, Universidade de Lisboa. November 2022

Abstract

Mesoporous silica nanoparticles (MSNs) feature unique characteristics that make them useful in many applications. Novel MSNs with a dual pore system, containing two distinct pore types that can carry and independently deliver different cargo selectively, would open even greater possibilities in fields such catalysis, sensing, energy, biomedicine, etc.

To develop dual pore system MSNs an innovative strategy is presented in this work based on a system of two surfactants that do not form mixed micelles and could be selective removed allowing selective pore functionalization and control release. Our objective was the development of novel cleavable surfactants that can be used as smart templates in the synthesis of MSNs and selectively removed through a specific stimulus. Two possible structures are proposed in this work: a light responsive surfactant and a redox responsive surfactant.

The redox responsive surfactant (CTAC-SS) was successfully obtained in moderate to high yields, and some preliminary studies confirm the potential to be used as smart surfactant. Degradability tests show that, after 30 minutes in the presence of dithiothreitol (DTT), occurs the cleavage of the S-S bonds, since it was possible to observe the characteristic absorption band of *ox*-DTT at 283 nm, which is a product of the reaction of DTT with the disulfide bond of CTAC-SS. An estimate critical packing parameter of CTAC-SS was obtained from its optimized structure, and the result indicate that CTAC-SS will form cylindrical micelles, due to the structure similarity with CTAB. Surface tension of a set of solutions of CTAC-SS was measured using the pendant drop method, however the results were not conclusive on the behavior of CTAC-SS in solution and was not possible to determine the critical micelle concentration (CMC). DLS results of CTAC-SS solutions reveal the presence of particles with 47 ± 5 nm of mean hydrodynamic diameter, which, if cylindrical micelles are formed as predicted by the cpp, correspond to the formation of cylindrical micelles with a maximum length of 261 nm.

Overall, the results indicate that our goal was achieved with the production of CTAC-SS, which can be a promising smart surfactant with broad applications, including the synthesis of dual pore MSNs and other nanostructures.

Keywords: mesoporous silica nanoparticles, dual pore system, stimuli responsive surfactant, selective template removal, selective functionalization

1. Introduction

Mesoporous Silica Nanoparticles (MSNs) are porous solid materials with inorganic siloxane structures and tunable pore diameters in the range of 2–50 nm.[1,2] MSNs are considered interesting materials in the nanotechnology field due to their unique characteristics that make them useful to employ in multiple fields.[2,3]

The possibility of creating silica nanoparticles with two types of pores that can interact independently with two different cargo seems attractive for applications in catalysis, sorption, separation, and biomedical fields.[4] It is possible to find in the literature some attempts to develop silica nanoparticles containing two different types of pores in their structure, however in all cases the templates used for the formation of the mesoporous structures were removed by calcination. This method removes all the surfactant organic molecules making it unsuitable to remove selectively the templates and thus selective pore functionalization is impractical, which limits the applications of these materials.

One possible alternative may rely on the use two surfactants where one of them can be selectively removed through a controlled stimulus (stimuli responsive surfactant). Cleavable surfactants contain

a bond that has intentionally been introduce between the hydrophilic part and the hydrophobic part and breaks down in a controlled way using a stimulus.[5] The cleavage of this bond will lead to one water-soluble and one water-insoluble product that can usually be removed by standard workup procedures, which is interesting for surfactants employed in numerous biochemical applications.[6]

The goal of this project is to synthesize a smart surfactant that should have a critical packing parameter (cpp) between 0.33-0.5 (to form cylindrical micelles), be stable under MSNs synthesis conditions (pH 9-11 and temperature close to 40ºC) and should not form mixed micelles with the inert surfactant.

Two surfactant structures were planned: a light responsive surfactant and a redox responsive surfactant. Both structures were designed to be structurally similar to cetyltrimethylammonium bromide (CTAB), which is commonly used as template for MSNs synthesis[7]: the polar group is a quaternary amine, and the hydrophobic group is defined to have the same number of atoms as the hydrophobic part of CTAB.

Finally, the behavior of the two molecules in solution was tested to find the best template to combine with an inert surfactant, for the synthesis of dual pore MSNs.

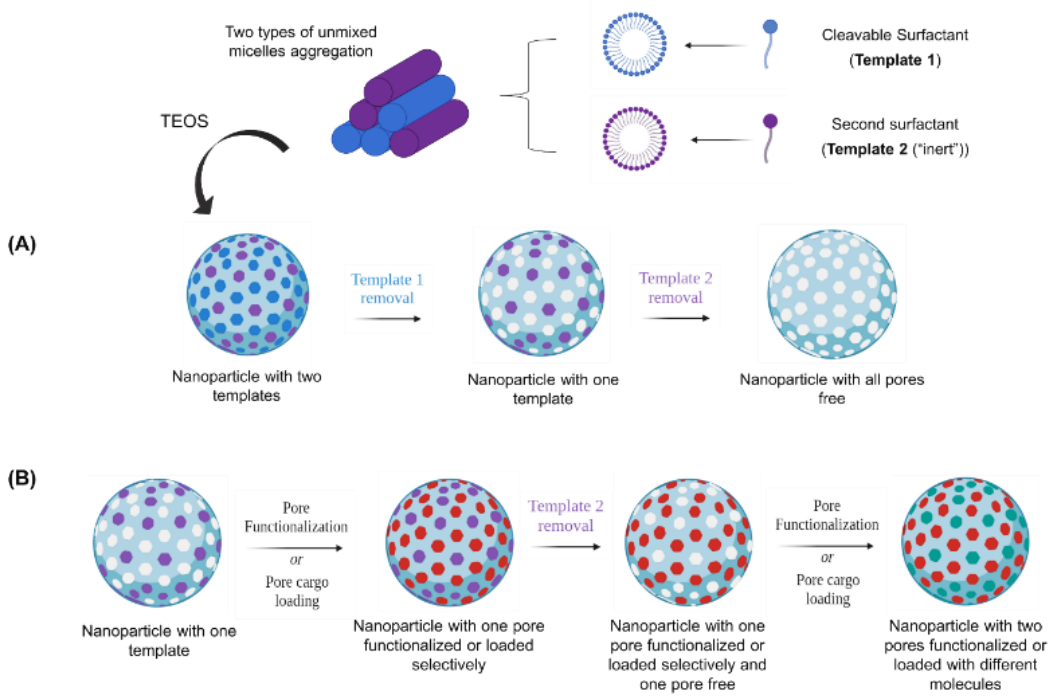

Figure 1. *Schematic representation of the strategy devised to produce a dual pore system MSN. A two-surfactant system containing a smart surfactant and a non-cleavable surfactant was designed to produce the dual-mesoporous structure enabling the selective removal of the templates (**A**). After the selective removal of each template the resulting free pores can be selective functionalized or loaded with different cargos (**B**).*

2. Materials and Equipment

All reagents and solvents were purchased from commercial suppliers without further purification except for dimethylformamide and tetrahydrofuran that were dried over molecular sieves. The following materials were used without further purification: iodomethane (≥99.0 %, Sigma-Aldrich), sodium hydride (dry, 90%, Sigma-Aldrich), (3-bromopropyl)trimethylammonium bromide (97%, Sigma-Aldrich), 1-Dodecanethiol (≥98%, Sigma-Aldrich), 1-bromohexane (≥98%, Sigma-Aldrich), 5-hydroxy-2-nitrobenzyl alcohol (97%, Sigma-Aldrich), cesium carbonate (99% Cs_2CO_3, Sigma-Aldrich), potassium carbonate (Sigma-Aldrich, ≥99%) , 2-dimethylaminoethanethiol hydrochloride (95%, Sigma Aldrich), Amberlite IRA-410 chloride form (Sigma-Aldrich), sodium hydroxide (Pure NaOH, PanReac AppliChem), tetrahydrofuran (ACS reagent, THF, Carlo Erb a Reagents), Dithiothreitol (97%, DTT, Sigma-Aldrich), methanol (Fisher Scientific, MeOH, ≥99.8%), ethyl acetate (Fisher Scientific, EtOAc, ≥99.8%), dimethylformamide (Fisher Scientific, DMF, ≥99.8%), acetonitrile (Fisher Scientific, MeCN,≥99.8%) and dichloromethane (99.95% DCM, José Manuel Gomes dos Santos, Lda). The deionized (DI) water was generated using a Millipore Milli-Q system (≥18 MΩcm, Merck, NJ, USA). PLC silica gel 60 F_{254} plates were purchase in Sigma-Aldrich. Evolution of reactions was followed by thin-layer chromatography (TLC) using silica gel 60 F_{254} Aluminium plates and revealed by UV light at 254 nm and 325 nm and, when needed, in an iodine chamber.

^{1}H NMR, ^{13}C NMR and ^{1}H -^{13}C HSQC spectra were acquired on a Bruker Avance III 400 (at 400.13 and 100.613 MHz) spectrometer. Deuterated solvents such as $CDCl_3$, MeOD and DMSO-d_6 were used. Chemical shifts (δ) and coupling constants (J) are expressed in ppm and in Hertz (Hz), respectively. ESI mass spectra were recorded on a LCQ Fleet mass spectrometer with an ESI source (Thermo Scientific) interfaced with an HPLC-DAD (Varian). ATR-FTIR spectra were recorded in the range of 4000–400 cm^{-1} on an Agilent Cary 630 FTIR spectrometer (Agilent Technologies). Raman spectra (Labram HR 800 Evolution, Horiba JobinYvon) was obtained with 532 and 633 nm excitation with a 600 grove/mm grating; laser power at the samples was ~10 mW and the unpolarized data were collected for 10s and 60s and 4 scans and 1 scan, at room temperature, using a 100x objective lens. CTAC-SS spectra was obtained with two different excitation wavelengths because the compound showed fluorescence when excited at 523 nm, thus the compound was excited at 633 nm from 1800 cm^{-1} to 3000 cm^{-1}. A Jasco V-660 UV-VIS Spectrophotometer (Oklahoma City, OK, USA) with a double monochromator and photomultiplier tube detector for higher resolution was used to record the absorption spectra. The measurements were carried out in 10 mm quartz cells at room temperature. Zetasizer Nano ZS (Malvern Instruments, UK), model ZEN3600, with 173º and 90º detector was used to determine the hydrodynamic diameters of the particles in solution, assuming Brownian movement.

3. Methods

3.1. Synthesis of novel stimuli responsive surfactants

3.1.1. Compound **1**

A mixture of 5-hydroxy-2-nitrobenzyl alcohol (300 mg, 1.77 mmol) and K_2CO_3 (735 mg, 5.31 mmol, 3 eq) was stirred in dry DMF (8 mL), for 1h at 60 °C under argon atmosphere. Bromohexane (0.37 mL, 2.655 mmol, 1.5 eq) was added dropwise to the reaction mixture and stirred for 3h at 60 °C under argon atmosphere. The reaction was monitored by TLC using hexane: EtOAc (2:1) as eluent. DMF was removed under reduced pressure. The resulting residue was dissolved in ethyl acetate and washed three times with water and brine. The organic phase was dried over $NaSO_4$, filtered, and evaporated under vacuum. The resulting product was obtained as a yellow-brown oil (440.6 mg, 98% yield). **^{1}H NMR** (400 MHz, $CDCl_3$) δ 8.19 (d, *J* = 9.1 Hz, 1H), 7.22 (d, *J* = 2.4 Hz, 1H), 6.89 (dd, *J* = 9.1, 2.6 Hz, 1H), 5.00 (s, 2H), 4.09 (t, *J* = 6.5 Hz, 2H), 1.87 – 1.80 (m, 2H), 1.52 – 1.45 (m, 2H), 1.38 – 1.36 (m, 4H), 0.93 (t, *J* = 6.8 Hz, 3H).**^{13}C NMR** (100 MHz, $CDCl_3$) δ 163.9, 140.2, 140.1, 128.1, 114.8, 113.6, 68.9, 63.1, 31.5, 28.9, 25.6, 22.6, 14.0.

3.1.2 Compound **2**

Compound **1** was dissolved in dry DMF, at 0 °C under argon atmosphere. Dry NaH was added portion-wise to the stirring reaction and after 10 minutes (3-bromopropyl)trimethylammonium bromide was added gradually to the reaction mixture and left to react for 1h at 0 °C and at least 1h at room temperature. The reaction was monitored by TLC using hexane: EtOAc (3:1) as eluent. The reaction was quenched with water and the aqueous phase was washed with EtOAc three times. The organic phases were combined and washed with a saturated Na_2CO_3 solution, brine and dried over anhydrous sodium bicarbonate. The reaction crude was purified by Preparative TLC plates using hexane: EtOAc (3:1) as eluent. Fractions from the preparative plate were scraped and the content of each fraction was extracted using organic solvents. Several changes were made to this protocol resulting in six unsuccessful attempts to synthesize the compound.

3.1.3 Compound **3**

2-(dimethylamino)ethanethiol hydrochloride (100 mg, 0.7059 mmol), 1-dodecanethiol (0.19 mL, 0.77649 mmol, 1.1 eq), Cs_2CO_3 (92 mg, 0.21177 mmol, 40 mol%) and CH_3CN (4 mL) were added to a 25 mL round bottom flask and the mixture was stirred under air at 60°C for 24 h. The reaction was monitored by TLC using dichloromethane/ methanol 5% as eluent. After cooling to room temperature, the solvent was evaporated under reduced pressure. Water was added (10 mL) to the resulting residue and the pH was increased until 8 by adding drops of a NaOH solution (0.5 M). The solution was washed with ethyl acetate two times. The organic phases were combined, dried over $NaSO_4$, filtered, and evaporated under vacuum.

The reaction crude was purified by Preparative TLC plates (dichloromethane/ methanol 5%) to give the desired product. The silica from the plates was scraped from the area corresponding to the stain of the desired product. The silica was placed on a Soxhlet, and the product extracted using ethyl acetate for 24h. The solvent was evaporated under reduced pressure to obtain the desired product (118.1 mg, 55% yield). **^{1}H NMR** (400 MHz, $CDCl_3$) δ 2.82 (t, *J* =

7.9 Hz 2H), 2.71 (t, *J* = 7.4 Hz, 2H), 2.63 (t, *J* = 6.8 Hz 2H), 2.29 (s, 6H), 1.72-1.65 (m, 2H), 1.41 – 1.27 (m, 18H), 0.89 (t, *J* = 6.7 Hz, 3H). **^{1}H NMR** (400 MHz, MeOD) δ 2.82 (t, *J* = 7.7, 2H), 2.75 – 2.67 (m, 4H), 2.31 (s, 6H), 1.74 – 1.67 (m, 2H), 1.48 – 1.31 (m, 20 H), 0.92 (t, *J* = 6.0 Hz, 3H).**^{13}C NMR** (100 MHz, $CDCl_3$) δ 58.8, 45.3, 39.2, 36.72 31.92 29.7, 29.7, 29.6, 29.6, 29.5, 29.4, 29.2, 29.2, 28.6, 22.7, 14.1. **ESI$^+$-MS** m/z 306.17 ($M+H^+$)

3.1.4. Compound **4**

A mixture of **3** (92.7 mg, 0.0965 mmol), excess of CH_3I and CH_3CN (6 ml) were added to a 25 mL round bottom flask and refluxed for 24 h at 95°C, under argon atmosphere. The solvent and excess of CH_3I were leaved to evaporate overnight inside the fume hood. The remaining solvent was removed in the vacuum line to give the redox sensitive surfactant (117.5 mg, 87% yield) as an orange solid. **^{1}H NMR** (400 MHz, MeOD) δ 3.78 (t, *J* = 8.6 Hz, 2H), 3.26 (s, 9H), 2.70 (t, *J* = 7.2 Hz, 2H), 1.74 – 1.66 (m, 2H), 1.44-1.32 (m, 18H), 0.92 (t, *J* = 6.6 Hz, 3H). **^{13}C NMR** (100 MHz, MeOD) δ 65.3, 52.7, 52.6, 52.6, 38.4, 31.7, 30.6, 29.4, 29.4, 29.3, 29.2, 29.1, 28.9, 28.8, 28.0, 22.3, 13.0. **ESI$^+$-MS** m/z 320.14 (M^+).

Compound **4** cation was change from iodine to chloride using an ionic exchange resin. 100 mg of compound **4** were added to a round bottom flask and methanol was added until the compound was completely dissolved. 197.12 mg of resin (Amberlite IRA-410 chloride form) were added to the mixture and left to stir for 24 h. The resin was filtered, and the solvent evaporated under pressure to obtain CTAC-SS. **^{1}H NMR** (400 MHz, MeOD) δ 3.75 (t, *J*= 8.6 Hz, 4H), 3.24 (s, 20H), 2.71 (t, *J* = 7.2 Hz, 2H), 1.73 – 1.66 (m, 2H), 1.46 – 1.32 (m, 18H), 0.92 (t, *J* = 5.9 Hz, 3H). **ESI$^+$-MS** m/z 320.14 (M^+).

3.2. Preliminary studies with CTAC-SS

3.2.1. Degradation studies for CTAC-SS

To perform the degradation studies, an aqueous solution of 2.5 mM of CTAC-SS and a 10mM aqueous solution of DTT were prepared and 1 mL of each solution was mixed (1.25 mM of CTAC-SS + 5 mM of DTT) in a quartz cuvette and the evolution over time of the absorption spectrum of the mixture was recorded in a Jasco V-660 UV-VIS spectrophotometer.

3.2.2. Determination of the critical micelle concentration (CMC) of CTAC-SS

The surface tension of a surfactant solution is linearly dependent on the logarithm of the concentration for low concentrations values. For concentrations above the CMC the surface tension remains constant with the increase of the concentration. The CMC value can be determined by the intersection of the fittings to the points in the two regimes. The surface tension can be measured using an Optical Tensiometer, that relies on the pendant drop method. Solutions of CTAC-SS with concentrations ranging from 0.05 to 3.5 mM were prepared in water at pH 7, measured and analysed using OneAttension software. Surface tension was measured 140 times to obtain the mean value and standard deviation for each concentration of CTAC-SS.

3.2.3. Computational studies

Geometry optimization of the cations of CTAB and CTAC-SS was performed using the electronic structure calculation program Gaussian 09 at the BLYP/6-31G (d,p) level of approximation in vacuum.[8] The calculation of the vibrational frequencies was used to confirm that a minimum in the potential energy surface (PES) was achieved (lack of imaginary frequencies). For both CTAB and CTAC-SS the initial structure for geometry optimization consisted in a planar chain of carbon (or carbon and sulphur) atoms in a zig-zag conformation. The optimized structures were analysed using Avogadro software (https://avogadro.cc/).

4. Results and discussion

The goal of this work was to develop mesoporous silica nanoparticles with a dual pore system. The strategy to obtain the desired particles involves a two-template system composed of a smart surfactant and an inert surfactant. This project focused on the synthesis of a light responsive surfactant and a redox responsive surfactant that were designed to be employed in the synthesis of dual pore MSNs as the stimuli responsive surfactant, taking into consideration the previously mentioned requirements. Afterwards, the smart surfactants must be evaluated to determine their behavior in solution and responsiveness to the respective stimulus. These results will determinate their potential as templates for the synthesis of the dual pore MSNs.

4.1. Synthesis and characterization of the light responsive surfactant

The desired photocleavable surfactant was prepared following a synthetic route of two steps (Figure 2) using as starting material the 5-hydroxy-2-nitrobenzyl alcohol.[9] The addiction of the hydrophobic part to the linker is made in the first step (compound **1**), and in a second step the hydrophilic part is added to the previous compound, resulting in the formation of the final molecule, compound **2**.

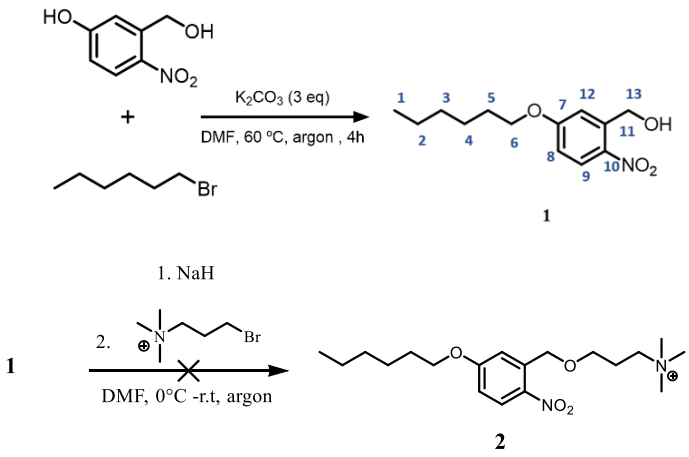

Figure 2. *Scheme for the synthesis of the light responsive surfactant (compound **2**).*

The ^{1}H NMR spectrum of compound shows three peaks corresponding to the three aromatic protons: two doublets at δ 8.19 (H_{C9}) (*J*= 9.1 Hz) and 7.22 ppm (H_{C12}) (*J*= 2.4 Hz) and one doublet of doublets at δ 6.89 ppm (H_{C8}) (*J*= 9.1, 2.6 Hz). Together with the information from ^{1}H - ^{13}C HSQC spectrum it was possible to assign the remaining protons to the respective carbons. The singlet located at δ 5 ppm integrates to two protons that are connected to C_{13} and the triplet located at δ 4.09 (*J* = 6.5 Hz) refers to the two protons linked to C_6. The multiplets integrating to two protons, at δ 1.87 – 1.80 and 1.52 – 1.45 ppm, and the multiplet located at δ 1.38 – 1.36 ppm that integrates to four protons, correspond to protons from the carbons in the alkyl chain. The three protons of C_1 appear as a triplet located at δ 0.93 ppm (*J* = 6.8 Hz).

The successful preparation of compound **1** was corroborated by the analysis of ^{13}C NMR and ^{1}H - ^{13}C HSQC spectra. The three quaternary carbons from the aromatic ring, C_7, C_{10} and C_{11}, are related to the peaks located at δ 163.9, 140.2 and 140.1 ppm. The remaining aromatic carbons are located at δ 128.1 (C_9), 114.8 (C_{12}) and 113.6 ppm (C_8). The peak related to carbon C_{13} is located at δ 63.1 ppm and the carbons from the alkyl chain are associated to signals at δ 68.9 (C_6), 31.5, 28.9, 25.6, 22.6, and 14.0 ppm (C_1). Compound **1** was analysed by ESI^{+}-MS, with a peak with high intensity appearing at m/z 214.26, but the results did not enable the identification of any compound. This does not imply that the compound was not produced, just means that it cannot be identified using this method.

To complete the synthesis of the photocleavable surfactant (compound **2**), compound **1** is dissolved in dry DMF at 0 ºC, under argon atmosphere, and NaH is added to remove the proton of the benzylic alcohol and allow the nucleophilic attack to the 3-bromopropyl trimethylammonium.[10] Six attempts were undertaken, however compound **2** was not obtained.

4.2. Synthesis and characterization of the redox responsive surfactant

The synthesis of the redox responsive surfactant was divided into two steps (Figure 3). The first step entails the formation of a disulfide bond between two different thiols, which results in the formation of an unsymmetrical disulfide. To do this, 2-(dimethylamino) ethanethiol and 1-dodecanethiol were reacted to give compound **3** by Base-Catalyzed Aerobic Oxidative Dehydrogenative Coupling. The second step is the methylation of the tertiary amine to give the quaternary ammonium salt (compound **4**).

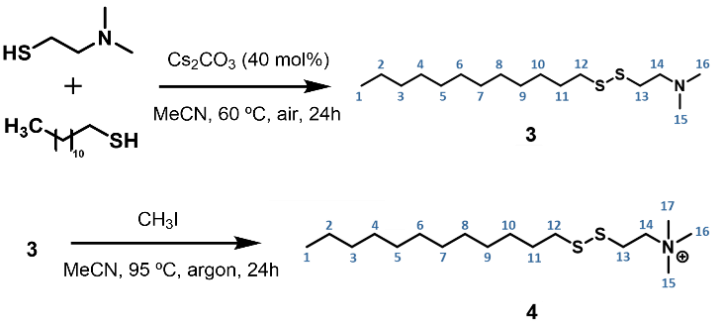

Figure 3. *Scheme for the synthesis of the redox responsive surfactant (compound **4**).*

The synthesis of compound **3** involves the heterocoupling of two different alkyl thiols, which is a difficult reaction to achieve. Song et al.[11] managed to obtain unsymmetrical disulfides resulting from the aerobic heterocoupling of functionalized alkyl thiols with tertiary butyl thiol or benzylic thiols catalysed by cesium carbonate, in moderate to high yields. This result encouraged us to devise a synthetic strategy based on their approach to synthesize the desired molecule. The two thiols selected for this work (2-(dimethylamino) ethanethiol hydrochloride (2-DAT) and 1-dodecanethiol) were combined with cesium carbonate (Cs_2CO_3), in acetonitrile. 40 mol% of catalyst were used, and after 24h at 60 °C the

compound was isolated in 55% yield, which is comparable to the results reported in the literature.

The ^{1}H NMR spectrum of the resulting product shows three triplets integrating to two protons each, located at δ 2.82 (*J* = 7.9 Hz), δ 2.71 (*J* = 7.1 Hz) and δ 2.63 ppm (*J* = 7.1 Hz) corresponding to carbon atoms number 12, 13, and 14, respectively, as confirmed by the ^{1}H - ^{13}C HSQC spectrum. The presence of the six protons corresponding to the two carbon atoms of the tertiary amine (15 and 16) is confirmed by the presence of a singlet at δ 2.29 ppm. The multiplet located at δ 1.72-1.65 ppm is associated to two protons that are connected to C_{11} and the multiplet located at δ 1.41-1.27 ppm corresponds to the 18 protons connected to carbon atoms from the alkyl chain with numbers from 2 to 10. The three protons connected to the last carbon from the alkyl chain (C_1) appear as a triplet at δ 0.89 ppm (*J* = 6.7 Hz). ^{13}C NMR and ^{1}H - ^{13}C HSQC spectra of compound **3** were analysed, and the peaks at δ 58.8 and 39.2 ppm were assigned to C_{14} and C_{13}, respectively. The carbons from the methyl groups connected to the amine (C_{15} and C_{16}) both appear at δ 45.3 ppm. The carbon from the hydrophilic group connected to the linker through a C-S bond, appear at δ 36.7 ppm (C_{12}). Moreover, the remaining peaks located at δ 29.7 (C_{11}), 31.9, 29.7, 29.6, 29.60, 29.5, 29.4, 29.2, 29.2 and 28.6 ($C_{3\text{-}10}$), 22.7 (C_2) and 14.1 ppm (C_1) were assigned to carbons from the alkyl chain. According to ESI^{+}-MS data, a peak at m/z 306.17, corresponding to the molecular ion $[M+H]^{+}$, confirms the formation of compound **3**.

To obtain compound **4** this, compound **3** was combined in acetonitrile with an excess of MeI, under reflux for 24h under argon atmosphere.[12] The excess of MeI and the solvent were evaporated inside the fume hood and the remaining solvent removed in the vacuum line, generating compound **4** in 87 % yield, most likely because of losses during compound recovery. The analysis of the ^{1}H NMR spectrum of compound reveals that all peaks integrate to the expected values. The protons connected to C_{13} from compound **4** appear on top of the deuterated solvent peak (MeOD), as concluded trough the analysis of the ^{1}H-^{13}C HSQC spectrum of compound **4**. A major indicator of the success of the methylation is the presence of a peak at δ 3.26 ppm that integrates to nine protons which agrees with the addition of another methyl group to the tertiary amine, forming the quaternary amine, which has three methyl groups and thus nine protons in the same chemical environment (H_{C15}, H_{C16} and H_{C17}). After quaternization of the amine, these peaks relocated to higher chemical shifts. The ^{13}C NMR spectrum of compound **4** does not differ from the ^{13}C NMR spectrum of compound **3**, as would be expected since their structures differ only in the presence of an extra methyl group, which is verified by the presence of three peaks in the ^{13}C NMR spectrum of compound **4** at δ 52.7, 52.6 and 52.6 ppm that are related to the three methyl groups (C_{15}, C_{16} and C_{17}) of the quaternary amine (surfactant polar group).

In conclusion, the surfactant was successfully synthesized, as evidenced by the result of the ESI^{+}-MS analysis, showing a peak at m/z 320.14 that corresponds to the molecular ion $[M]^{+}$.

After successfully synthesizing compound **4**, an ionic exchange was performed to replace the iodine counterion with chlorine, to improve the compound's water solubility. After the ionic exchange, a whitish solid was obtained, with a yield of 83% (due to losses during the experimental procedure). The compound, denominated CTAC-SS, was analysed by ^{1}H NMR and ESI^{+}-MS techniques. The ^{1}H NMR spectrum of CTAC-SS has the same profile as the spectrum of compound **4**. In the ESI^{+}-MS spectrum of CTAC-SS appears a high intensity peak at m/z 273.05, that could not be attributed to any known fragment, but is also present in the ESI^{+}-MS spectrum of compound **4**. The peak that corresponds to the molecular ion $[M]^{+}$ (m/z 320.24) is also present in the ESI^{+}-MS spectrum of CTAC-SS. This data together with the NMR analysis allows us to assume that the compound remains intact during the ion exchange.

CTAC-SS was analysed by ATR-FTIR and Raman spectroscopy to confirm the presence of the disulfide bond (-S-S-) in the compound's structure. In the infrared spectra of 2-(dimethylamino) ethanethiol hydrochloride (2-DAT) (Figure 4A) it is possible to see the characteristic peak of the thiol group (-SH) at 2560 cm^{-1},[13] that is not present in the spectrum of CTAC-SS (Figure 4B).

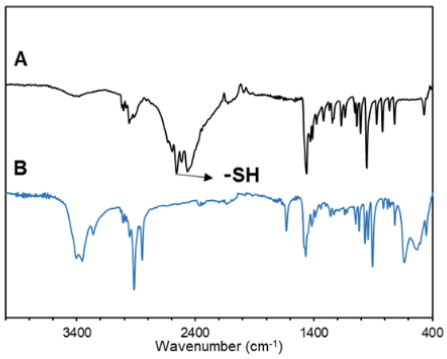

Figure 4. *ATR-FTIR spectra of 2-DAT (A) and CTAC-SS (B).*

In the Raman spectrum of CTAC-SS appears a clear Raman signal at 511 cm^{-1} (Figure 5A) which is related to the presence of a disulfide bond in the

molecule. As expected, a signal at 2577 cm^{-1} (-SH) is present in the spectrum of 1-dodecanethiol (Figure 5C), and no signal related to the thiol group appears in the spectrum of CTAC-SS (Figure 5B).[14]

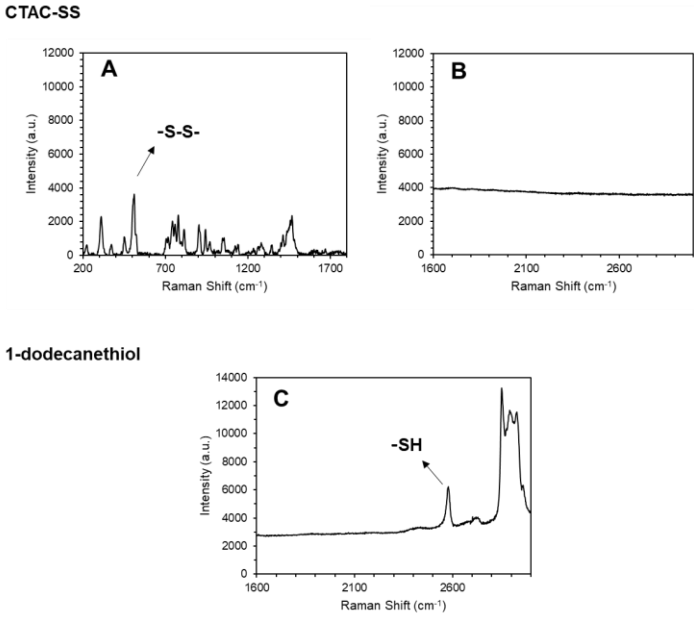

Figure 5. *Raman spectra of CTAC-SS - 532 nm excitation (A) and 633 nm excitation (B)- and 1-dodecanethiol (C).*

These results confirm the presence of a disulfide bond in CTAC-SS and eliminate the possibility of contamination with the starting materials, thus reinforcing the success of the synthesis of compound **4**, and confirming the success of the ionic exchange, which culminates in the formation of CTAC-SS.

4.3. Preliminary results with CTAC-SS

4.3.1. Degradation studies for CTAC-SS

Aqueous solutions of CTAC-SS (2.5 mM) and DTT (10 mM) were prepared at pH 7. The absorption of the mixture (1.25 mM of CATAC-SS + 5 mM of DTT) was recorded at a fixed wavelength (λ= 283 nm), where the characteristic absorption band of *ox*-DTT appears, each 2 s for 30 minutes and the results are compiled in Figure 6A. Absorbance increases until it reaches a constant value, that corresponds to the complete cleavage of all disulfide bonds present in solution, confirming that DTT can be used to degrade our surfactant. After 30 min an absorption spectrum of the mixture was recorded, where is possible to visualize the characteristic absorption band of *ox*-DTT (Figure 6B). The absorption spectrum of the CTAC-SS aqueous solution (1.25 mM) at pH 7 is also shown in (Figure 6B), to prove that the isolated compound is not responsible for the band at 283 nm, which appears only in the presence of DTT.

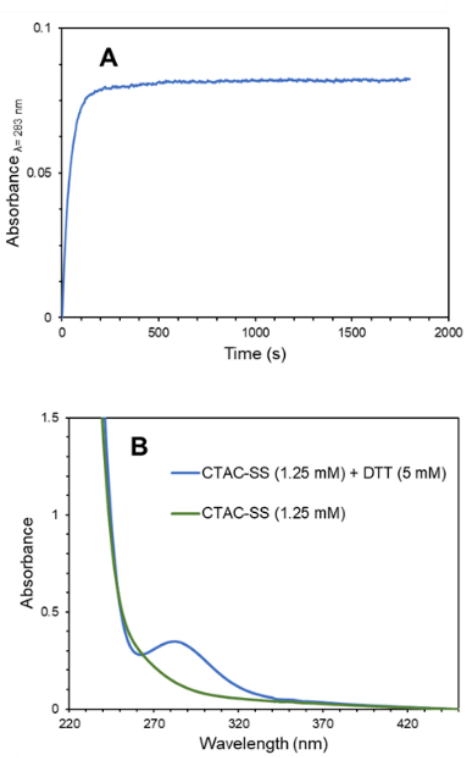

Figure 6. *Absorbance at λ= 283 nm over 30 minutes of an aqueous solution of CTAC-SS (1.25 mM) and DTT (5 mM), at pH 7 (A); Absorption spectrum of an aqueous solution of CTAC-SS (1.25 mM) and DTT (5 mM) at pH 7, after 30 minutes, and an aqueous solution of CTAC-SS (1.25 mM) at pH 7(B).*

4.3.2. Computational studies

Geometry optimization of CTAB and CTAC-SS were performed and from the obtained optimized structures it was possible to make an approximate calculation of the critical packing parameter (cpp) of both surfactants.

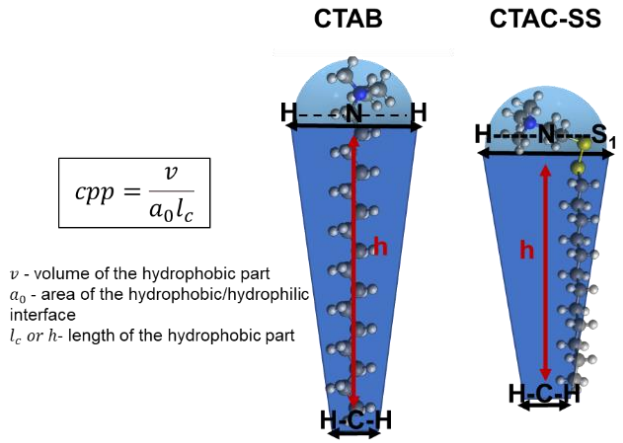

Figure 7. *Schematic representation of the method used to calculate the critical packing parameter (cpp) of CTAB (left) and CTAC-SS (righ).*

The value obtained for CTAB was 0.53, which is higher than expected since CTAB forms cylindrical

micelles (0.33<cpp<0.5), and for CTAC-SS was 0.46, indicating that this surfactant will also form cylindrical micelles.

4.3.3. Determination of the critical micelle concentration (CMC) of CTAC-SS

The mean surface tension values were plotted as a function of the logarithm of the concentration of CTAC-SS (0.05- 3.5 mM) (Figure 8). A decrease in surface tension was expected with log ([CTAC-SS]) until the value corresponding to the CMC was reached, with constant surface tension above the CMC. However, the CTAC-SS results were not as expected. Surface tension remained constant as concentration increased up to 3.5 mM. These results allow us to speculate on possible behaviors of CTAC-SS in solution. One hypothesis is the existence of a very high CMC, therefore the chosen concentration range would be far below the CMC, where little adsorption at the surface would be observed. On the other hand, the practically unchanged surface tension could be explained by a very low CMC, with the formation of micelles at very low concentrations, but without surfactant adsorption to the air-water interface.

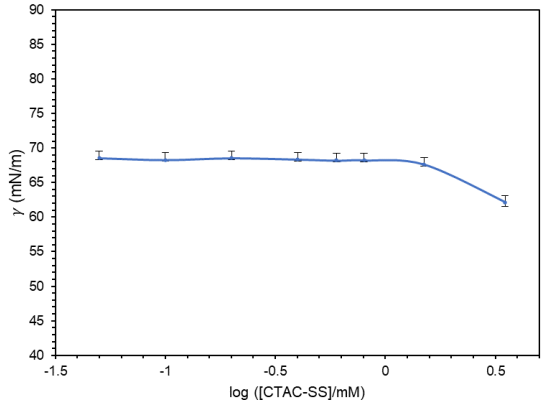

Figure 8. *Surface tension of CTAC-SS as a function of the logarithm of the concentration.*

4.3.4. Dynamic Light Scattering

Dynamic Light Scattering of CTAC-SS solutions was performed to check if there was any self- assembling of the CTAC-SS, and to obtain the hydrodynamic diameter of the formed structures. The correlograms and the results of the size distribution by number are shown in Figure 9 and Figure 10, respectively. Trought the analysis of the correlogram of CTAC-SS dispersions with concentrations 1.67 mM, 1 mM, 0.8 mM, and 0.6 mM, it is possible to conclude that all dispersions are polydisperse, since the decay of the correlation curve is extended in all cases, which indicates larger polydispersity of the samples. Moreover, the size distribution by number of each solution has only one peak, meaning that in solution there is only a population of particles with similar diameters. The mean hydrodynamic diameter of the particles present in CTAC-SS dispersions is 47 ± 5 nm, which indicates that the particles present in the solutions with different concentrations have consistent sizes, and although the surface tension results indicate that there is no adsorption at the surface, there seems to exist formation of micelles in solution.

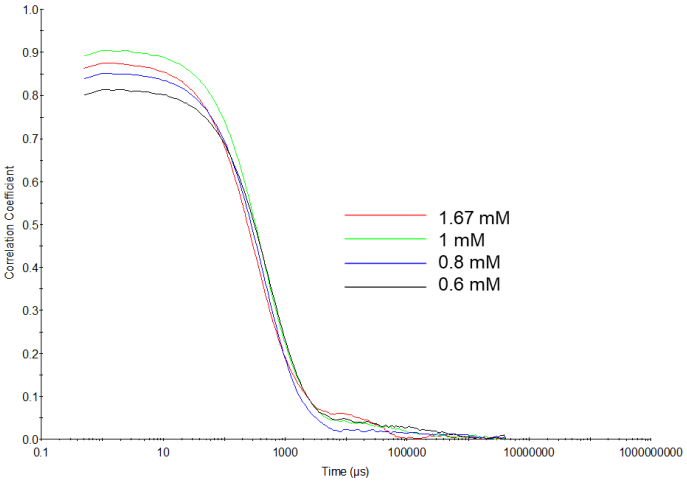

Figure 9. *Correlogram of CTAC-SS solutions: 1.67 mM, 1 mM, 0.8 mM, and 0.6 mM.*

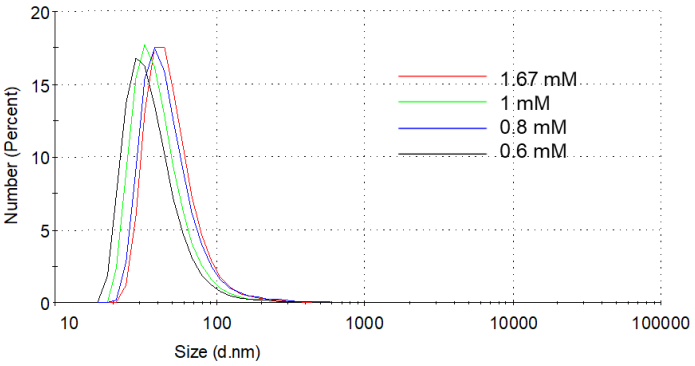

Figure 10. *Size distribution by number of CTAC-SS solutions: 1.67 mM, 1 mM, 0.8 mM, and 0.6 mM.*

Considering the formation of cylindrical micelles, the radius of the micelle (R) can be defined as the length of the hydrophobic part (2 nm) and the length (L) of the micelle can be determined through the relationship between the hydrodynamic radius (R_H) and the radius of gyration (R_g). (Equations 1 and 2).[15,16]

$$\frac{R_g}{R_H} = \frac{1}{\sqrt{3}} \ln\left(\frac{L}{2R} - 0.5\right) \quad (1)$$

$$R_g{}^2 = \frac{R^2}{2} + \frac{L^2}{12} \quad (2)$$

The value obtained for the length of the micelle was 261 nm, considering a rigid structure (fully stretched). The micelle length is then lower than 261 nm since the micelle can be in a wormlike conformation (not a rigid cylinder).

5. Conclusions

The goal of this work was to design a novel smart surfactant with hydrophilic and hydrophobic moieties that are cleavable in response to a stimulus. This surfactant would satisfy the necessary conditions to integrate the two-surfactant system used in the strategy for the synthesis of dual pore MSNs. A light responsive surfactant and a redox responsive surfactant were chosen, and simple synthetic schemes were devised to obtain both molecules in just two steps.

The synthesis of the light sensitive surfactant was not successful, because of the instability of the substrate during the second step of the synthesis. In the case of the redox responsive surfactant, the product was successfully synthesized in two steps. The intermediate and the final molecule were obtained in moderate to high yields and characterized by ^{1}H NMR, ^{13}C NMR, HSQC spectroscopy and by ESI^{+}-MS.

After successfully synthesizing the iodine salt of the redox responsive surfactant, an ionic exchange was undertaken to replace the iodine counterion with chlorine to increase the compound's solubility in water, originating a whitish solid in high yield, denominated CTAC-SS. This compound was characterized by ^{1}H NMR, ESI^{+}-MS, ATR-FTIR and Raman, proving its integrity during the ionic exchange.

Some preliminary studies with CTAC-SS were conducted to evaluate its behavior as a smart surfactant. Geometry optimization of CTAB and CTAC-SS were performed, and the critical packing parameter (cpp) values of both surfactants were estimated. The cpp obtained for CTAB was 0.53 and for CTAC-SS was 0.46, which indicate that using the same approximations for the calculation of the cpp for both molecules, the results are similar despite the differences in their structure. Most probably, CTAC-SS will form cylindrical micelles. Degradability tests were conducted, and the results show that CTAC-SS disulfide bond suffers cleavage in the presence of dithiothreitol (DTT). After 30 minutes in the presence of the reducing agent, it was possible to observe the characteristic absorption band of *ox*-DTT at 283 nm, which is an indicator of the degradability of CTAC-SS. The surface tension of solutions of CTAC-SS was measured using the pendant drop method. The surface tension did not change within the range of 0.05- 3.5 mM CTAC-SS concentrations. These results were not conclusive on the behavior of CTAC-SS in solution, and it was not possible to calculate de CMC of CTAC-SS from the plot of surface tension as a function of the logarithm of the concentration. Possible explanations are that either the molecule does not absorb to the liquid-gas interface but forms micelles; or the CMC is very high (out of the range tested). However, DLS results of CTAC-SS solutions reveal the presence of particles with 47 ± 5 nm of mean hydrodynamic diameter, which, if cylindrical micelles are formed as predicted by the cpp, correspond to the formation of cilyndrical micelles with a maximum length of 261 nm.

The overall results highlight the success of this work and indicate that CTAC-SS can be a promising smart surfactant with broad applications, such as in the synthesis of dual pore MSNs and other nanostructures. Nonetheless, the preliminary results still leave some questions to be clarified about the behavior of CTAC-SS as a surfactant, which can be addressed by conducting additional research and refining previous studies.

In future work, it would be interesting to verify the formation of MSNs using this surfactant as template, and later combine it with an inert surfactant to produce the desired dual pore MSNs. The strategy is to use CTAC-SS, an alkyl cleavable surfactant, together with a perfluorinated "inert" surfactant, such as HFDePC[17], taking advantage of the poor miscibility of the fluorocarbon and hydrocarbon chains, thus avoiding the formation of mixed micelles.[17]

6. Reference

(1) Rastegari, E.; Hsiao, Y. J.; Lai, W. Y.; Lai, Y. H.; Yang, T. C.; Chen, S. J.; Huang, P. I.; Chiou, S. H.; Mou, C. Y.; Chien, Y. An Update on Mesoporous Silica Nanoparticle Applications in Nanomedicine. *Pharmaceutics* **2021**, *13* (7), 1–56. https://doi.org/10.3390/pharmaceutics13071067.

(2) Pal, N.; Lee, J.-H.; Cho, E.-B. Recent Trends in Morphology-Controlled Synthesis and Application of Mesoporous Silica Nanoparticles. *Nanomaterials* **2020**, *10* (11), 2122. https://doi.org/10.3390/nano10112122.

(3) Wu, S. H.; Lin, H. P. Synthesis of Mesoporous Silica

Nanoparticles. *Chem. Soc. Rev.* **2013**, *42* (9), 3862–3875. https://doi.org/10.1039/c3cs35405a.

(4) Niu, D.; Ma, Z.; Li, Y.; Shi, J. Synthesis of Core-Shell Structured Dual-Mesoporous Silica Spheres with Tunable Pore Size and Controllable Shell Thickness. *J. Am. Chem. Soc.* **2010**, *132* (43), 15144–15147. https://doi.org/10.1021/ja1070653.

(5) Brown, P.; Butts, C. P.; Eastoe, J. Stimuli-Responsive Surfactants. *Soft Matter* **2013**, *9* (8), 2365–2374. https://doi.org/10.1039/c3sm27716j.

(6) Holmberg, K. Surfactants with Controlled Half-Lives. *Curr. Opin. Colloid Interface Sci.* **1996**, *1* (5), 572–579. https://doi.org/10.1016/s1359-0294(96)80094-x.

(7) Yamamoto, E.; Kuroda, K. Colloidal Mesoporous Silica Nanoparticles. *Bull. Chem. Soc. Jpn.* **2016**, *89* (5), 501–539. https://doi.org/10.1246/bcsj.20150420.

(8) M. J. Frisch, G. W. Trucks, H. B. Schlegel, G. E. Scuseria, M. A. Robb, J. R. Cheeseman, G. Scalmani, V. Barone, B. Mennucci, G. A. Petersson, H. Nakatsuji, M. Caricato, X. Li, H. P. Hratchian, A. F. Izmaylov, J. Bloino, G. Zheng, J. L. Sonnenberg, M. Had, and D. J. F. Gaussian 09. Gaussian, Inc.: Wallingford CT 2009.

(9) Ho, H. T.; Phan, T. N. T.; Bonnevide, M.; Malicki, N.; Couty, M.; Jestin, J.; Gigmes, D. Photolabile Well-Defined Polystyrene Grafted on Silica Nanoparticle via Nitroxide-Mediated Polymerization (NMP). *Macromol. Rapid Commun.* **2021**, *42* (18), 1–5. https://doi.org/10.1002/marc.202100181.

(10) Picchetti, P.; Dimarco, B. N.; Travaglini, L.; Zhang, Y.; Ortega-Liebana, M. C.; De Cola, L. Breaking with Light: Stimuli-Responsive Mesoporous Organosilica Particles. *Chem. Mater.* **2020**, *32* (1), 392–399. https://doi.org/10.1021/acs.chemmater.9b03937.

(11) Qiu, X.; Yang, X.; Zhang, Y.; Song, S.; Jiao, N. Efficient and Practical Synthesis of Unsymmetrical Disulfides: Via Base-Catalyzed Aerobic Oxidative Dehydrogenative Coupling of Thiols. *Org. Chem. Front.* **2019**, *6* (13), 2220–2225. https://doi.org/10.1039/c9qo00239a.

(12) Shao, H.; Jiang, L.; Meng, W.-D.; Qing, F.-L. Synthesis and Antimicrobial Activity of a Perfluoroalkyl-Containing Quaternary Ammonium Salt. *J. Fluor. Chem.* **2003**, *124* (1), 89–91. https://doi.org/10.1016/S0022-1139(03)00193-3.

(13) Cheng, Y.-J.; Zhang, A.-Q.; Hu, J.-J.; He, F.; Zeng, X.; Zhang, X.-Z. Multifunctional Peptide-Amphiphile End-Capped Mesoporous Silica Nanoparticles for Tumor Targeting Drug Delivery. *ACS Appl. Mater. Interfaces* **2017**, *9* (3), 2093–2103. https://doi.org/https://doi.org/10.1021/acsami.6b12647.

(14) Zhai, H.; Wang, Y.; Wang, M.; Liu, S.; Yu, F.; Gao, C.; Li, G.; Wu, Q. Construction of a Glutathione-Responsive and Silica-Based Nanocomposite for Controlled Release of Chelator Dimercaptosuccinic Acid. *Int. J. Mol. Sci.* **2018**, *19* (12), 3790. https://doi.org/https://doi.org/10.3390/ijms19123790.

(15) Hammouda, B. Analysis of the Beaucage Model. *J. Appl. Crystallogr.* **2010**, *43* (6), 1474–1478. https://doi.org/https://doi.org/10.1107/S0021889810033856.

(16) Chu, B. *Laser Light Scattering: Basic Principles and Practice*; Courier Corporation, 2007.

(17) Canadas, C. Hybrid Nanocontainer with Dual Control Release System, Universidade de Lisboa, 2021.